SIGNAL AND IMAGE PORT OUTPUT POWER IN THE QUANTUM THEORY OF MIXING

Qing Ke and M. J. Feldman

Department of Electrical Engineering
University of Rochester, Rochester, NY 14627

ABSTRACT

The quantum theory of mixing is essential for the *interpretation* of experimental superconducting quasiparticle (SIS) mixers. When the bias and tuning parameters are known, the theory is quite successful at predicting the mixer performance, gain and noise temperature. However, the theory usually predicts much higher conversion gain for some other set of bias and tuning parameters, and this is not seen in experiment. Thus the theory is less useful for engineering *design* of SIS mixers. We believe we have resolved this longstanding discrepancy. We find there are two distinct "optimum" operation modes for ideal SIS mixers. The high gain mode predicted by the theory will not be accessible in real experiments. To understand this, we present the equations of a DSB SIS mixer in a novel form, in terms of the complex-plane phase angle between the amplitude modulation input admittance vector and the local oscillator input admittance vector.

INTRODUCTION

Classical mixer theory does not apply to heterodyne mixers operating at a frequency ω high enough that the voltage scale of the resistive nonlinearity is smaller than $\hbar\omega/e$. The quantum theory of mixing [1] developed by J.R. Tucker must be used. Tucker's theory is very successful in describing the superconductor-insulator-superconductor (SIS) quasiparticle mixer. In particular, if the operating parameters of an optimized mixer can be independently determined, the theory predicts the IF conversion gain quite precisely [2,3].

Yet there is a major discrepancy between the theory's predictions and the experiments. From the earliest attempts [4], the best SIS mixers have had low to moderate conversion gain (as high as 10 dB in two experiments [5,6]), but *optimized* computer fits to these experiments often predict very high to infinite gain. In fact, it appears that for some set of bias and tuning parameters the quantum theory of mixing always predicts considerably higher conversion gain for high quality SIS junctions than can actually be achieved in experiment. This is true even when harmonic effects and saturation are taken into account.

One clear early example of this is Ref. [7]. There the highest conversion gain achieved was 4.3 dB, and the theory reasonably predicted that value using measured operating parameters. However, the theory also predicted conversion gain higher than 20 dB for a different set of operating parameters. In this experiment the junction capacitance was large, so harmonic effects could be safely ignored.

We believe we have resolved this longstanding mystery. We find there are two distinct and disjoint "optimum" operation modes for ideal SIS mixers which are predicted by the quantum theory of mixing. One mode has very high or infinite IF conversion gain, and the "reflected" power (the signal reflection gain and the signal-to-image conversion gain) is extremely high as well. The other mode has moderate IF conversion gain, but the reflection gains tend to be very small. The high reflected power implies that the high gain mode will not be accessible in real experiments. Therefore, eliminating the high gain solution in computer simulations should give much better agreement with experiments.

CALCULATIONS

In a typical experiment the gain of an SIS mixer is maximized by varying the dc bias, the LO power, the embedding impedances, etc. When this procedure is attempted in calculations, however, the quantum theory of mixing predicts infinite gain for high quality SIS junctions over a wide range of parameter values. There is no unique optimum bias point. To avoid this difficulty, and to make our calculation as realistic as possible, we take as our figure of merit not the gain but the minimum value of the SSB (single sideband) receiver noise temperature

$$T_R = T_M + T_{IF}/\mathcal{G}_{IF} . \qquad (1)$$

Thus our calculation involves a trade-off between minimizing the mixer noise temperature T_M and maximizing the mixer conversion gain $\mathcal{G}_{IF}$, which is mediated by the noise temperature of the IF amplifier T_{IF}.

The equations used to calculate T_R are taken from Ref. [1]. Only a few are presented here. We consider a DSB (double sideband: equal signal and image termination) mixer in the three-frequency low-IF approximation, which should be a fairly good representation of most well-designed experimental mixers. For a DSB mixer the thermal noise from the image termination does not affect receiver optimization, so for convenience we assume zero physical temperature and the thermal noise simply reduces to the quantum noise temperature of the mixer, $\hbar\omega/2k$. We ignore the thermal noise from the IF termination which is reflected from the mixer back into the IF amplifier, although this can be an important factor for real SIS receivers. We ignore any interference from the Josephson effect.

The standard SSB IF conversion gain of a DSB SIS mixer (Ref. [1], Eq. 4.74) can be written in the novel form:

$$\mathcal{G}_{IF} = \frac{G_L G_{01}^2}{(G_{00}+G_L)^2} \frac{4G_S}{|(Y_S+Y_S')\cos\theta|^2}, \tag{2}$$

$$Y_S' = G_S' + jB_S' \equiv G_{11} + G_{1-1} - \frac{2G_{01}G_{10}}{G_{00}+G_L} + j\left(B_{11} + B_{1-1} - \frac{2G_{01}B_{10}}{G_{00}+G_L}\right). \tag{3}$$

$\mathcal{G}_{IF}$ depends upon $Y_S = G_S + jB_S$, the source admittance seen by the SIS junction at the signal and the image frequencies, and upon the load conductance G_L which represents the conductance of the IF amplifier circuitry as seen by the junction. The explicit dependence of $\mathcal{G}_{IF}$ upon Y_S in Eq. 2 is given by a simple impedance matching formula which has its maximum at $Y_S = |G_S'| - jB_S'$. Note that G_S', which can be negative, is <u>not</u> the input conductance of our mixer. (Y_S' is the input admittance in the simple amplitude modulation model of the SIS mixer, in which the signal results from an amplitude modulation of the LO, as described in Ref. [1], Sec. III.B.) The input admittance of the mixer at the local oscillator frequency ω is

$$Y_{LO}^{\circ} \equiv I_{LO}/V_{LO} = G_{LO}^{\circ} + jB_{LO}^{\circ} = G_{11} - G_{1-1} + j(B_{11} - B_{1-1}), \tag{4}$$

where I_{LO} is the (complex) amplitude of the current and V_{LO} is the (real) amplitude of the voltage across the junction at frequency ω. Of course $G_{LO}^{\circ} > 0$. $\mathcal{G}_{IF}$ also depends upon Y_S, implicitly, through the angle θ. θ is the relative phase angle between the vectors (Y_S+Y_S') and

$(Y_S+Y_{LO}^{\circ})$ in the complex plane. Thus $|(Y_S+Y_S')|\cos\theta$ is the projection of the vector (Y_S+Y_S') in the direction of $(Y_S+Y_{LO}^{\circ})$.

Equations 2 - 4 are expressed in terms of the elements of the small-signal admittance matrix [1], $Y_{ij} = G_{ij} + jB_{ij}$. Each G_{ij} is evaluated as an infinite sum over index n of the currents $I_n \equiv I_{dc}(V_n)$ weighted by a combination of Bessel functions of argument $\alpha \equiv eV_{LO}/\hbar\omega$, where $I_{dc}(V)$ is the unmodulated dc I-V characteristic of the SIS junction, $V_n \equiv V_0 + n\hbar\omega/e$, and V_0 is the dc bias voltage.

We pay close attention to the reflected power. The signal reflection gain and the signal-to-image conversion gain of a DSB mixer in the three-frequency low-IF approximation are respectively:

$$\mathcal{G}_S = \frac{1}{4\cos^2\theta}\left|\frac{Y_S - Y_S'^*}{Y_S + Y_S'} + \frac{Y_S - Y_{LO}^{\circ *}}{Y_S + Y_{LO}^{\circ}}\right|^2, \tag{5}$$

$$\mathcal{G}_I = \frac{1}{4\cos^2\theta}\left|\frac{Y_S^* - Y_S'}{Y_S + Y_S'} - \frac{Y_S^* - Y_{LO}^{\circ}}{Y_S + Y_{LO}^{\circ}}\right|^2. \tag{6}$$

Note that the explicit dependence of $\mathcal{G}_S$ and $\mathcal{G}_I$ upon Y_S is given by the interference of two voltage reflection coefficients. Although high IF conversion gain might seem advantageous in the context of Eq. 1, when $\mathcal{G}_{IF}$ is infinite both $\mathcal{G}_S$ and $\mathcal{G}_I$ (and in fact the output power at all sideband frequencies [8]) are infinite as well, clearly an unstable situation. In this paper we will show that the IF conversion gain can be sizable even if an SIS mixer is operated far from instability, with very small reflected power.

There has been little appreciation of $\mathcal{G}_S$ and $\mathcal{G}_I$ in the literature. An exception is Ref. [9], which enforced an approximate signal input impedance match. But a preliminary version of the present paper [10] is the first to mention the signal-to-image conversion gain of an SIS mixer in any context.

To simplify our calculations we will ignore all reactances: in Eqs. 2 - 6 each admittance Y is replaced by its conductance G, and $\cos\theta = 1$. This entails the controversial assumption that the quantum susceptance has no significant effect. It has recently been argued that the quantum susceptance is a central element of the behavior of SIS mixers [11]. Nevertheless, we believe that this nonlinear reactance has little effect on the performance of an optimized SIS receiver except insofar as it affects LO impedance matching. This question will be further addressed below.

We calculated the minimum noise temperature of the SIS receiver at each frequency. At each frequency the optimum values of G_S, V_0, and α were calculated given discrete values for the remaining parameters and an assumed SIS junction I-V curve. We have performed these calculations for a wide range of parameters, but only a few illustrative results are presented here. We normalize voltages to the energy gap voltage V_g, conductances to the normal state resistance R_N, and frequencies to the energy gap frequency $\omega_g \equiv eV_g/\hbar$.

RESULTS

The dotted curve of Fig. 1 shows the minimum theoretical noise temperature of an SIS receiver for frequencies up to $\omega = 0.2\ \omega_g$, using an SIS I-V curve corresponding to the best experimental junctions (see Ref. [12], Fig. 1, "sharp"), with $G_L = 0.3/R_N$, $T_{IF} = 3$ K, and $V_g = 3$ mV. The smoothness of this curve hides the fact that it includes two distinct and disjoint types of behavior. The thick lines in Fig. 2 represent the three corresponding small-signal gains. It is seen that $\mathcal{G}_{IF}$ is extremely high, and $\mathcal{G}_S$ and $\mathcal{G}_I$ are even higher, for normalized frequencies between 0.03 and 0.12. For other frequencies $\mathcal{G}_{IF}$ is more moderate but still sizable, while $\mathcal{G}_S$ and $\mathcal{G}_I$ are quite small.

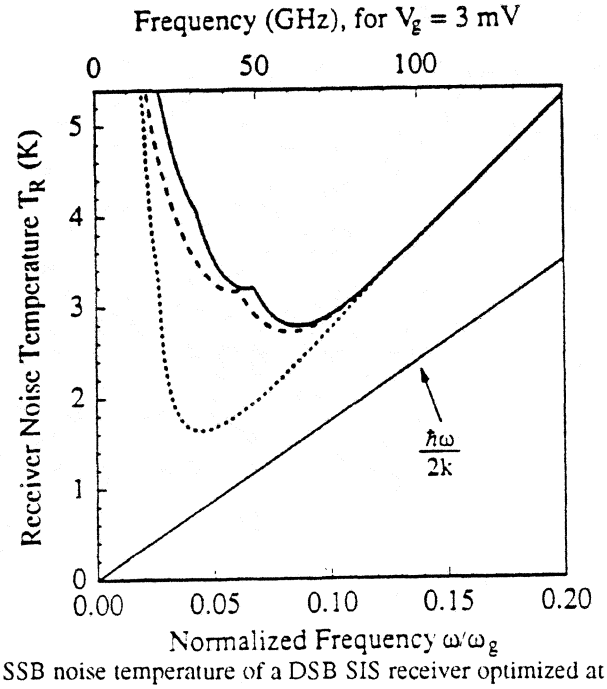

Fig. 1. The SSB noise temperature of a DSB SIS receiver optimized at each frequency. The computation assumes a sharp I-V curve, $G_L = 0.3/R_N$, $T_{IF} = 3$ K, and $V_g = 3$ mV. The dotted curve is the universal minimum of T_R, the dashed curve is calculated with the constraint $G_s' > 0$, and the solid curve is calculated with the constraint $\mathcal{G}_I \leq 1/4$.

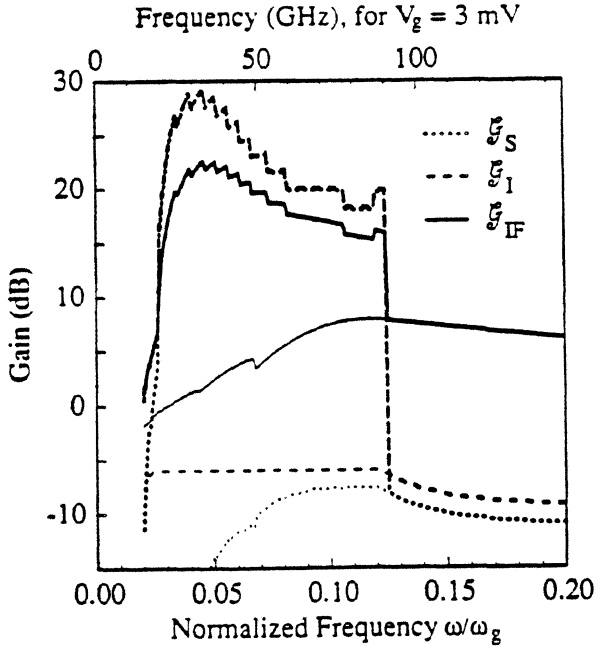

Fig. 2. The thick lines represent the IF conversion gain $\mathcal{G}_{IF}$, the signal reflection gain $\mathcal{G}_S$, and the signal-to-image conversion gain $\mathcal{G}_I$, which correspond to the dotted curve of Fig. 1. The thin lines represent the gains which correspond to the solid curve of Fig. 1.

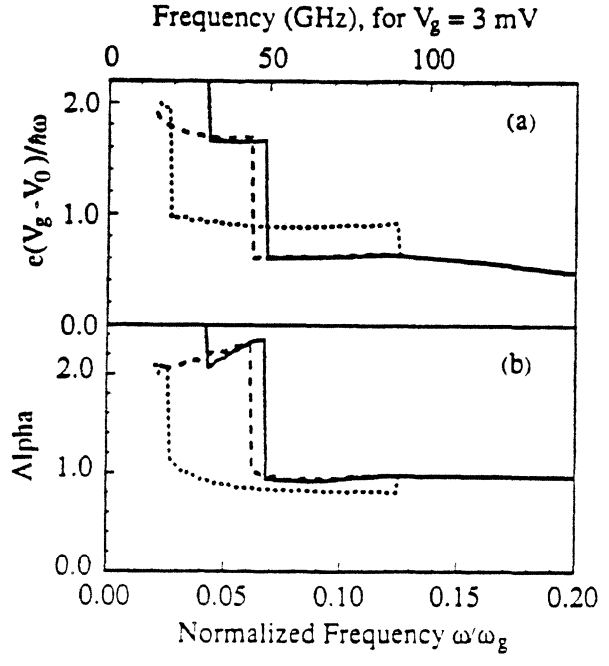

Fig. 3. Bias voltages for the optimized receiver of Fig. 1. a) The dc bias voltage presented in units of "photon step number" (see Eq. 7), b) The normalized LO voltage amplitude $\alpha \equiv eV_{LO}/\hbar\omega$. The three line styles correspond to those of Fig. 1.

We performed the same receiver optimization calculations subject to the constraint $\mathcal{G}_I \leq 1/4$. In other words, we eliminate all results giving significant output power at the image frequency. This results in the solid curve of Fig. 1 and the thin lines in Fig. 2. It is clear that the reflected power constraint eliminates the high gain operating mode and so the moderate gain mode extends continuously across the entire frequency region.

This illustrates a general feature of our results: For a wide range of parameter values there are two distinct minima for T_R corresponding to two distinct receiver operation modes. One mode has very high IF conversion gain, and the reflected power is very high as well. The other has moderate IF conversion gain, but the reflected power tends to be very small.

Figures 3 and 4 show that the bias and tuning parameters are very different for the two modes. As a measure of the dc bias voltage V_0 we define the non-integer generalization of the photon step number,

$$N_{step} \equiv e(V_g - V_0)/\hbar\omega, \tag{7}$$

so that $0 < N_{step} < 1$ can be called the "first photon step," etc. Fig. 3a shows that the moderate gain mode is well approximated by $N_{step} \approx 0.6$ on the first photon step. At lower frequencies the optimum bias point moves to the second photon step and the moderate gain mode has $N_{step} \approx 1.6$. This behavior continues to lower frequency and is in fact a general feature of our results: The optimum dc bias voltage for the moderate gain operating mode (for low frequency) is always slightly below the middle of a photon step. For the high gain mode, however, $N_{step} \geq 0.9$ on the first photon step and 1.9 on the second photon step.

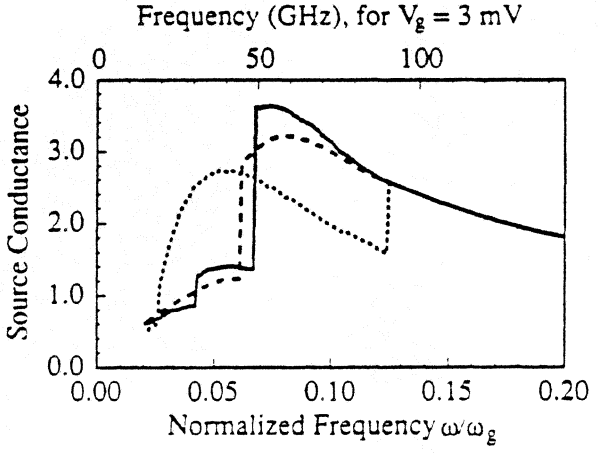

Fig. 4. The normalized source conductance $G_S R_N$ for the optimized receiver of Fig. 1. The three line styles correspond to those of Fig. 1.

Again, this is a general feature of our results: The optimum dc bias voltage for the high gain mode (unlike most experiments) is always at the beginning of a photon step. Fig. 3b shows that the frequency dependence of α is quite similar to that of N_{step}.

The source conductance G_S for minimum noise temperatures is also very different for the two modes (Fig. 4). For the high gain mode G_S is almost exactly equal to $-G_S'$, as required by Eq. 2. The G_S for the moderate gain mode, however, has a very different character; it is quite close to the value which minimizes the shot noise, and this in turn follows closely the LO input conductance G_{LO} [12]. Note that the optimum source conductance is in every case experimentally convenient: G_S is roughly of order $1/R_N$.

It is instructive to consider the mixer output conductance, G_L°, of our optimized receiver (Fig. 5). The high gain mode generally but not exclusively has negative G_L°. The moderate gain mode always occurs with positive G_L°. Note that in the lower half of the frequency range of Fig. 5 the output impedance match is surprisingly good.

An important general feature of our results is that the moderate gain mode is quite insensitive to the level of reflected power allowed. In fact, for the parameters used for Figs. 1 to 5, *any* reasonable constraint on the maximum allowed $\mathcal{P}_I$, from 0.1 to 10, serves to eliminate the high gain mode but has very little effect on the moderate gain mode. This is persuasive evidence that these two operating modes are indeed distinct. [This explains why the $G_S' > 0$ -constrained case (dashed lines in Figs. 1, 3, 4, and 5) lies quite close to the reflected-power-constrained case (solid lines).]

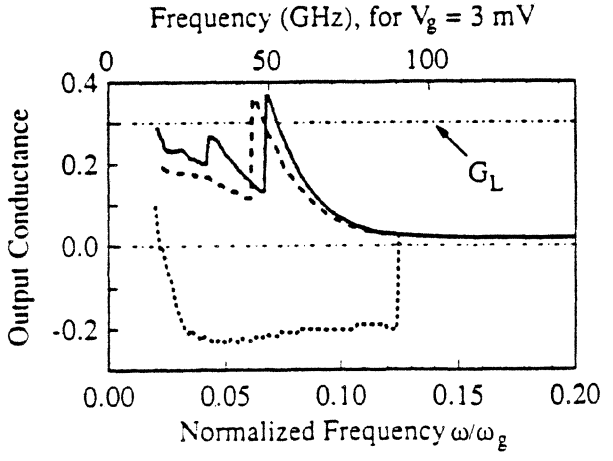

Fig. 5. The normalized output conductance $G_L^\circ R_N$ for the optimized receiver of Fig. 1. The three line styles correspond to those of Fig. 1. The load conductance $G_L = 0.3/R_N$ is also shown.

The behavior we have described is quite widespread. In fact, if we had chosen a larger value for T_{IF}, if we had assumed some leakage current, if we had included the quantum susceptance in generating Figs. 1 to 5, the high gain mode would predominate over a much wider frequency range.

DISCUSSION

We understand our results in the following way. T_M and $\mathcal{G}_{IF}$ in Eq. 1 are in general slowly varying functions of their various parameters. The exception is that when G_S' is negative the quantity G_S+G_S' can go to zero, giving analytically infinite $\mathcal{G}_{IF}$ in Eq. 2. Near exact cancellation occurs over only a small region of parameter space. Thus we can picture a display of T_R in a multi-parameter space as having a rather sharp minimum near $G_S+G_S' = 0$ and more gradual behavior, including a broad minimum, elsewhere. These two minima correspond to our two operating modes. Near $G_S+G_S' = 0$ both $\mathcal{G}_S$ and $\mathcal{G}_I$ will be very large (cf. Eqs. 5 and 6). If the vicinity of $G_S+G_S' = 0$ is forbidden (by constraining $\mathcal{G}_I$), the remaining minimum will be quite insensitive to the operating parameters.

This analysis supports our conclusion that, were we to include the quantum susceptance and a tuning susceptance in our calculations, the result would be very much the same. Equation 2 shows two possibilities for analytically infinite $\mathcal{G}_{IF}$. First, Y_S+Y_S' can go to zero. But even if $G_S' > 0$, it is possible for the vector (Y_S+Y_S') to be perpendicular to $(Y_S+Y_{LO}^\circ)$, giving $\cos\theta = 0$. This means that the quantum susceptance widens the range of possibility of infinite gain in SIS mixers (as noted in Ref. [11]), so that infinite gain can be predicted for instance for poorer quality I-V curves and over a wider frequency range. Nevertheless, the discussion of the above paragraph still exactly applies, but for the quantity $(Y_S+Y_S')\cos\theta$ rather than G_S+G_S'. Thus considering the quantum susceptance underlines the importance of removing the high gain solutions in computer simulations.

In Fig. 2 that $\mathcal{G}_I$ is always larger than $\mathcal{G}_S$. This is true for all of our simulations: for an optimized SIS receiver there is always more power returned to the source at the image frequency than at the signal frequency! We do not know the physical reason for this. Mathematically, it is clear from inspection of Eqs. 5 and 6 that this is a simple consequence of the fact that the optimum G_S is always intermediate between G_{LO}° and G_S'. In fact $\mathcal{G}_S$ can be extremely small while $\mathcal{G}_I$ is still sizable; an example is seen at low frequencies in Fig. 2. Thus the signal-to-image gain $\mathcal{G}_I$ is a crucial parameter.

It is clear that the high gain mode should not be experimentally accessible. The very large returned power makes the mixer extraordinarily sensitive to small variations in the signal and image terminations. The high output power (at higher sideband frequencies as well, unless they are perfectly terminated) is extremely conducive to mixer saturation. The sensitivity of the high gain mode to mixer operating parameters implies that these solutions are near instability and will be obliterated by noise and other processes. It appears that the high gain mode is a mere mathematical curiosity, forgoing a direct experimental assault.

On the other hand, we show that it is possible to have moderately high gain, 8 dB for the particular example of Fig. 2, for stable mixer operation with low noise and very low returned power. We believe that this resolves the mystery outlined in the Introduction. Since the high gain mode is not accessible, constraining the reflected power in computer fitting should give much better agreement with experiments..

CONCLUSION

It is important to consider the signal reflection gain and especially the signal-to-image conversion gain in computer simulations of SIS mixers. The computed minimum receiver noise temperature often entails extremely high signal and image returned power, and this type of solution is likely inaccessible in real experiments. If this mode of operation is eliminated, it is possible to have moderately high gain with very low returned power and low noise temperature, as seen in experiment.

Acknowledgment: This work was supported in part by NSF grant # AST-8922301.

REFERENCES

[1] J.R. Tucker and M.J. Feldman, "Quantum detection at millimeter wavelengths," *Rev. Mod. Phys.* 57, 1055-1113 (Oct. 1985).

[2] M.J. Feldman, S.-K. Pan, A.R. Kerr, and A. Davidson, "SIS mixer analysis using a scale model," *IEEE Trans. Magnetics* MAG-19, 494-497 (May 1983).

[3] C.A. Mears, Qing Hu, P.L. Richards, A.H. Worsham, D.E. Prober, and A.V. Räisänen, "Quantum limited quasiparticle mixers at 100 GHz," *IEEE Trans. Magnetics* MAG-27, 3363-3369 (March 1991).

[4] T.-M. Shen, P.L. Richards, R.E. Harris, and F.L. Lloyd, "Conversion gain in mm-wave quasiparticle heterodyne mixers," *Appl. Phys. Lett.* 36, 777-779 (1 May 1980).

[5] A.V. Räisänen, D.G. Crété, P.L. Richards, and F.L. Lloyd, "A 100 GHz SIS mixer with 10 dB coupled gain," in *1987 IEEE MTT-S Int. Microwave Symp. Dig.*, 929-930.

[6] J.A. Carpenter, A.D. Smith, E.R. Arambula, L.P.S. Lee, T. Nelson, and L. Yujiri, "100 GHz SIS mixer with improved rf matching," *IEEE Trans. Magnetics* MAG-27, 2654-2657 (March 1991).

[7] W.R. McGrath, P.L. Richards, A.D. Smith, H. van Kempen, R.A. Batchelor, D.E. Prober, and P. Santhanam, "Large gain, negative resistance, and oscillations in superconducting quasiparticle heterodyne mixers," *Appl. Phys. Lett.* 39, 655-658 (Oct. 1981).

[8] M.J. Feldman, "Some analytical and intuitive results in the quantum theory of mixing," *J. Appl. Phys.* 53, 584-592 (Jan. 1982).

[9] A.R. Kerr and S.-K. Pan, "Some recent developments in the design of SIS mixers," *Int. J. Infrared Millimeter Waves* 11, 1169-1187 (Oct. 1990).

[10] Qing Ke and M.J. Feldman, "Reflected power effects in computer simulations using the quantum theory of mixing," in *1992 IEEE MTT-S Int. Microwave Symp. Dig.*, 1425-1428.

[11] C.A. Mears, Qing Hu, and P.L. Richards, "The effect of the quantum susceptance on the gain of superconducting quasiparticle mixers," *IEEE Trans. Magnetics* MAG-27, 3384-3387 (March 1991).

[12] Qing Ke and M.J. Feldman, "Optimum source conductance for high frequency superconducting quasiparticle receivers," *IEEE Trans. Microwave Theory Tech.* MTT-41, 600-605 (April 1993).